Measurements of the proton generalized polarizabilities

Nikos Sparveris[1,*]

[1]Temple University, Department of Physics, Philadelphia, PA 19122, USA

Abstract. The EM polarizabilities characterize a fundamental property of the proton that involves the system's response to an external electromagnetic (EM) field. They describe how easily the charge and magnetization distributions inside the system are distorted by the EM field, such as during the Compton scattering with a real photon. When the polarizabilities are generalized to finite momentum transfer by replacing the incoming real photon of the Compton scattering process with a space-like virtual photon, they map out the deformation of the quark densities in a proton subject to an EM field. Recent experimental measurements at Jefferson Lab have provided high precision data, that offer guidance and present significant challenges to nuclear theory. Future experiments aim to improve further these measurements, both by extending their kinematic range as well as by improving the level of the experimental precision.

1 Introduction

The polarizabilities [1] are fundamental structure constants for any composite system, like the proton. The two scalar polarizabilities - the electric, α_E, and the magnetic, β_M - can be interpreted as the response of the proton's structure to the application of an external electric or magnetic field, respectively. They describe how easily the charge and magnetization distributions inside the proton are distorted by the EM field and provide the net result on the system's spatial distributions. In order to measure the polarizabilities, one must generate an electric ($\vec{E}$) and a magnetic ($\vec{H}$) field. In the case of the proton, this is provided by the photons in the Compton scattering process. The two scalar polarizabilities appear as second order terms in the expansion of the real Compton Scattering (RCS) amplitude in the energy of the photon. A simplistic description of the polarizabilities can be provided through the resulting effect of an electromagnetic perturbation applied to the nucleon constituents. An electric field moves positive and negative charges inside the proton in opposite directions. The induced electric dipole moment is proportional to the electric field, and the proportionality coefficient is the electric polarizability which quantifies the stiffness of the proton. On the other hand, a magnetic field has a different effect on the quarks and on the pion cloud within the nucleon, giving rise to two different contributions in the magnetic polarizability, a paramagnetic and a diamagnetic contribution, respectively. The generalization [2] of the two scalar polarizabilities in four-momentum transfer space, $\alpha_E(Q^2)$ and $\beta_M(Q^2)$, is an extension of the static electric and magnetic polarizabilities obtained in RCS. The GPs are studied through measurements of the virtual Compton scattering (VCS) process [2] γ^*p→ pγ. The VCS is accessed experimentally through the ep→epγ reaction, where the incident real photon of the RCS process is

---

[*] e-mail: sparveri@temple.edu

replaced by a virtual photon. The virtuality of the incident photon (Q^2) sets the scale of the observation and allows one to map out the spatial distribution of the polarization densities in the proton, while the outgoing real photon provides the EM perturbation to the system. The meaning of the GPs is analogous to that of the nucleon form factors. Their Fourier transform will map out the spatial distribution density of the polarization induced by an EM field. They probe the quark substructure of the nucleon, offering unique insight to the underlying nucleon dynamics, and they frequently enter as input parameters in various scientific problems e.g. in the hadronic two-photon exchange corrections, which are needed for a precise extraction of the proton charge radius from muonic Hydrogen spectroscopy measurements [3].

2 Experimental measurements of the generalized polarizabilities

The early MAMI, JLab and Bates VCS experiments [4, 5, 8, 9, 28, 29], two decades ago, shaped a first understanding of the proton electric and magnetic GPs. These measurements contradicted the naive Ansatz of a single-dipole fall-off for $\alpha_E(Q^2)$, pointing out to an enhancement at low Q^2, evidenced by two independent experiments [4, 5]. The magnetic generalized polarizability measurements were characterized by large uncertainties, highlighting the challenges in extracting the small magnetic polarizability signal. The precision of the measurements was significantly improved a few years later during the follow-up MAMI experiment [6, 7, 30], that utilized the high resolution spectrometers setup in A1 and explored the region Q^2=0.10 GeV^2 to 0.45 GeV^2.

The most recent measurements involve the VCS-I experiment [10] at the Thomas Jefferson National Accelerator Facility. The data were acquired in Hall C of Jefferson Lab. Electrons with energies of 4.56 GeV at a beam current up to 20 μA were produced by Jefferson Lab's Continuous Electron Beam Accelerator Facility (CEBAF) and were scattered from a 10 cm long liquid-hydrogen target. The Super High Momentum Spectrometer (SHMS) and the High Momentum Spectrometer (HMS) of Hall C were used to detect in coincidence the scattered electrons and recoil protons, respectively. The experiment focused on the region Q^2=0.28 GeV^2 to 0.40 GeV^2, with a special interest in the puzzling measurements of $\alpha_E(Q^2)$ that were reported at Q^2=0.33 GeV^2 [4, 5]. The experiment capitalized on the unique capabilities of the experimental setup in Hall C at Jefferson Lab that allow to conduct measurements of the scalar GPs with an unprecedented precision. Furthermore, cross section measurements were conducted for azimuthally symmetric kinematics in the photon angle, since measurements of the cross section asymmetry enhances further the sensitivity in the extraction of the polarizabilities, and suppresses part of the systematic uncertainties. Overall, a significant improvement was accomplished in the precision of the extracted generalized polarizabilities compared to previous measurements. The extracted electric and magnetic GPs are shown in Fig. 1. The measurements point to a local enhancement of $\alpha_E(Q^2)$ in the measured region, at the same Q^2 as previously reported in [4, 5], but with a smaller magnitude than what was originally suggested. The Q^2-dependence of the electric GP has been explored using methods that employ both traditional fits to the data using predefined functional forms, as well that are based on a data-driven technique that assumes no direct underlying functional form [10]. Both methods point to a Q^2-dependence for $\alpha_E(Q^2)$ that is consistent with the presence of a structure in the measured region, in sharp contrast with the current theoretical understanding that suggests an $\alpha_E(Q^2)$ that decreases monotonically with increasing Q^2.

The theory predictions cover a wide range of approaches such as chiral effective field theories [14–19], the linear σ-model [20, 21], the Effective Lagrangian Model [22], relativistic [23] and nonrelativistic [24, 25] constituent quark models. The $\beta_M(Q^2)$ is expected to have a smaller magnitude relative to $\alpha_E(Q^2)$. This can be explained by the competing paramagnetic and diamagnetic contributions in the proton, which largely cancel. For $\beta_M(Q^2)$, the

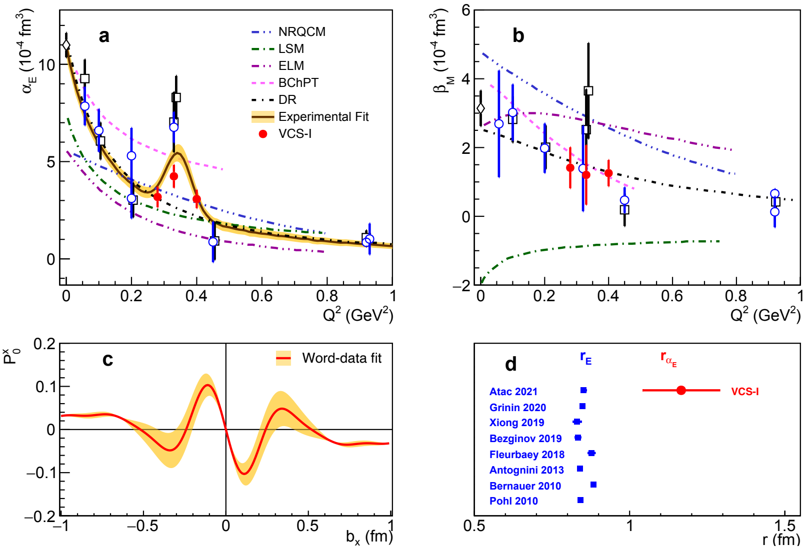

Figure 1. The generalized polarizabilities of the proton
a) The electric generalized polarizability measured in VCS-I (red circles). The world data [4–9, 27–30] (open-symbols) are shown for results that involve the Dispersion-Relations (circle) and Low-Energy-Expansion analysis (box). The theoretical calculations of BChPT [14], NRQCM [25], LSM [20], ELM [22] and DR [11–13] are also shown. **b)** The magnetic generalized polarizability. **c)** Induced polarization in the proton when submitted to an EM field as a function of the transverse position with photon polarization along the x axis for $b_y = 0$. The x-y defines the transverse plane, with the z axis being the direction of the fast moving protons. **d)** The proton electric polarizability radius $r_{\alpha_E} \equiv \sqrt{\langle r^2_{\alpha_E} \rangle}$. The measurements of the proton charge radius r_E [31–38] (blue points) are shown for comparison.

results point to a smooth Q^2-dependence and the near-cancellation of the paramagnetic and the diamagnetic contributions in the proton at $\sim Q^2$=0.4 GeV^2. The theoretical predictions for the two generalized polarizabilities vary noticably, and the VCS-I results impose strict constraints, providing new input to the theory.

The generalized polarizabilities data allow to derive the spatial deformation of the quark distributions in the proton subject to the influence of an external electromagnetic field [26], as shown in Fig. 1(c). Furthermore, they allow to extract the electromagnetic polarizability radii of the proton, similarly to the procedure that is followed for the extraction of the proton electric charge radius from the form factor measurements. For the mean square electric polarizability radius it is found that $\langle r^2_{\alpha_E} \rangle = 1.36 \pm 0.29\ fm^2$, a value that is considerably larger compared to the mean square charge radius of the proton, $\langle r^2_E \rangle \sim 0.7\ fm^2$ [1]. The dominant contribution to this effect is expected to arise from the deformation of the mesonic cloud in the proton under the influence of an external EM field. For the extraction of the mean square magnetic polarizability radius from the magnetic polarizability measurements one can derive $\langle r^2_{\beta_M} \rangle = 0.63 \pm 0.31\ fm^2$.

3 Future Experiments

The beamtime for the next phase of the VCS experiment at Jefferson Lab (VCS-II) has been approved by the JLab PAC51 (E12-23-001) [40]. The measurements will take place in Hall

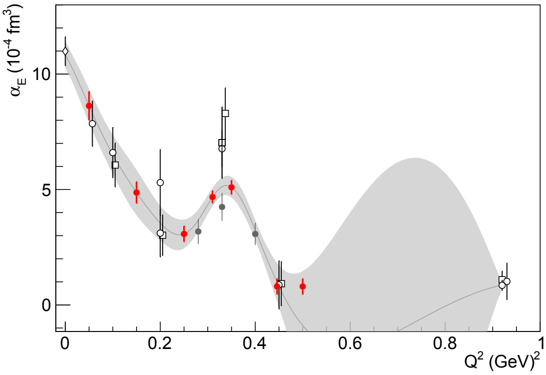

Figure 2. The VCS-II projected measurements for α_E (red circles). The world data are shown as black points (the VCS-I results are indicated with filled gray circles).

C, employing a similar experimental setup as in VCS-I, namely the SHMS and the HMS spectrometers, and will require 62 days of beam-on-target with a $E_\circ = 1.1\ GeV$ and $2.2\ GeV$ electron beam at I=75 μA and a 10 cm liquid hydrogen target. The projected measurements of the VCS-II are shown in Fig. 2.

The recent measurements of the electric GP highlight the importance of employing alternative experimental methods for the measurement of the polarizabilities. The use of polarized and positron beams provides an alternative, powerful avenue to access the proton GPs [41]. The lepton beam charge (e) and polarization (λ) dependence of the $lp \to lp\gamma$ differential cross section is given by $d\sigma^e_\lambda = d\sigma_{\mathrm{BH}} + d\sigma_{\mathrm{VCS}} + \lambda\, d\tilde{\sigma}_{\mathrm{VCS}} + e\,(d\sigma_{\mathrm{INT}} + \lambda\, d\tilde{\sigma}_{\mathrm{INT}})$, where $d\sigma$ ($d\tilde{\sigma}$) are the polarization independent (dependent) contributions which are even (odd) functions of the azimuthal angle ϕ. The $d\sigma_{\mathrm{INT}}$ involves the real part of the VCS amplitude that contains the GP effects, while $d\tilde{\sigma}_{\mathrm{INT}}$ is proportional to the imaginary part of the VCS amplitude which does not depend on the GPs. Combining lepton beams of opposite charge and different polarization enables the complete separation of the four unknown INT and VCS contributions. More specifically, using unpolarized electron and positron beams, one can construct the unpolarized beam-charge asymmetry (BCA) A^C_{UU} as

$$A^C_{UU} \quad = \quad \frac{(d\sigma^+_+ + d\sigma^+_-) - (d\sigma^-_+ + d\sigma^-_-)}{d\sigma^+_+ + d\sigma^+_- + d\sigma^-_+ + d\sigma^-_-} = \frac{d\sigma_{\mathrm{INT}}}{d\sigma_{\mathrm{BH}} + d\sigma_{\mathrm{VCS}}}.$$

With polarized lepton beams, one can construct the lepton beam-spin asymmetry (BSA)

$$A^e_{LU} \quad = \quad \frac{d\sigma^e_+ - d\sigma^e_-}{d\sigma^e_+ + d\sigma^e_-} = \frac{d\tilde{\sigma}_{\mathrm{VCS}} + e d\tilde{\sigma}_{\mathrm{INT}}}{d\sigma_{\mathrm{BH}} + d\sigma_{\mathrm{VCS}} + e\, d\sigma_{\mathrm{INT}}}.$$

The theoretical groundwork and a first theoretical exploration for the potential of this type of measurements has been conducted in [41], indicating that the BCA and the BSA asymmetries exhibit significant sensitivity to both scalar GPs. A combination of both types of assymmetries, is powerful towards separating the contribution from the $d\tilde{\sigma}_{\mathrm{VCS}}$ and $d\tilde{\sigma}_{\mathrm{INT}}$ terms, offering both sensitivity to the GPs as well as a cross-check of the unitarity input in the dispersive formalism, as discussed in [41]. A Letter-of-Intent for the measurement of the polarizabilities using this method was submitted to the JLab PAC51 (LOI12-23+001) and the collaboration has received the recommendation to proceed with the submission of a full proposal.

References

[1] Zyla, P. A. *et al.* Review of Particle Physics. *Prog. Theor. Exp. Phys.* **2020**, 083C01 (2020).

[2] Fonvieille, H., Pasquini, B. and Sparveris, N. Virtual Compton Scattering and Nucleon Generalized Polarizabilities. *Prog. Part. Nucl. Phys.* **113**, 103754 (2020).

[3] Pasquini, B. and Vanderhaeghen, M. Dispersion Theory in Electromagnetic Interactions *Annu. Rev. Nucl. Part. Sci.* **68**, 75-103 (2018).

[4] Roche, J. *et al.* First Determination of Generalized Polarizabilities of the Proton by a Virtual Compton Scattering Experiment *Phys. Rev. Lett.* **85**, 708-711 (2000).

[5] Janssens, P. *et al.* A new measurement of the structure functions PLL-PTT/ε and PLT in virtual Compton scattering at $Q^2 = 0.33(GeV/c)^2$ *Eur. Phys. J.* **A37**, 1-8 (2008)

[6] Beričič, J. *et al.* New Insight in the Q^2 Dependence of Proton Generalized Polarizabilities *Phys. Rev. Lett.* **123**, 192302 (2019)

[7] Fonvieille, H. *et al.* Measurement of the generalized polarizabilities of the proton at intermediate Q^2 *Phys. Rev. C* **103**, 025205 (2021)

[8] Laveissiere, G. *et al.* Measurement of the Generalized Polarizabilities of the Proton in Virtual Compton Scattering at $Q^2 = 0.92$ and 1.76 GeV^2 *Phys. Rev. Lett.* **93**, 122001 (2004)

[9] Fonvieille, H. *et al.* Virtual Compton scattering and the generalized polarizabilities of the proton at $Q^2 = 0.92$ and 1.76 GeV^2 *Phys. Rev. C* **86**, 015210 (2012)

[10] R. Li, et al., Nature 611, 265 (2022)

[11] Pasquini, B., Drechsel, D.,Gorchtein, M., Metz, A., and Vanderhaeghen, M. Dispersion relation formalism for virtual Compton scattering and the generalized polarizabilities of the nucleon *Phys. Rev. C* **62**, 052201(R) (2000).

[12] Pasquini, B., Gorchtein, M., Drechsel, D., Metz, A. and Vanderhaeghen, M. Dispersion relation formalism for virtual Compton scattering off the proton *Eur. Phys. J. A* **11**, 185 (2001).

[13] Drechsel, D., Pasquini, B. and Vanderhaeghen, M. Dispersion relations in real and virtual Compton scattering *Phys. Rep.* **378**, 99 (2003).

[14] Lensky, V., Pascalutsa, V. and Vanderhaeghen, M. Generalized polarizabilities of the nucleon in baryon chiral perturbation theory *Eur. Phys. J. C* **77**, 119 (2017).

[15] Hemmert,T. R., Holstein, B., Knochlein G., Scherer S. Virtual Compton scattering off the nucleon in chiral perturbation theory *Phys. Rev. D* **55**, 2630 (1997).

[16] Hemmert, T. R., Holstein, B., Knochlein, G., Scherer, S. Generalized polarizabilities and the chiral structure of the nucleon *Phys. Rev. Lett.* **79**, 22 (1997).

[17] Hemmert, T. R., Holstein, B., Knochlein, G., Drechsel, D. Generalized polarizabilities of the nucleon in chiral effective theories *Phys. Rev. D* **62**, 014013 (2000).

[18] Kao, C. W., Vanderhaeghen, M. Generalized spin polarizabilities of the nucleon in heavy baryon chiral perturbation theory at next-to-leading order *Phys. Rev. Lett.* **89**, 272002 (2002).

[19] Kao, C. W., Pasquini, B., Vanderhaeghen, M. New predictions for generalized spin polarizabilities from heavy baryon chiral perturbation theory *Phys. Rev. D* **92**, 119906 (2015).

[20] Metz, A., Drechsel, D. Generalized polarizabilities of the nucleon studied in the linear sigma model *Z. Phys. A* **356**, 351 (1996).

[21] Metz, A., Drechsel, D. Generalized polarizabilities of the nucleon studied in the linear sigma model. 2 *Z. Phys. A* **359**, 165 (1997).

[22] Korchin, A.and Scholten, O. Nucleon polarizabilities in virtual Compton scattering *Phys. Rev. C* **58**, 1098 (1998)

[23] Pasquini, B. and Salme, G. Nucleon generalized polarizabilities within a relativistic constituent quark model *Phys. Rev. C* **57**, 2589 (1998).

[24] Liu, G. Q., Thomas, A. W., Guichon, P. A. M. Virtual Compton scattering from the proton and the properties of nucleon excited states *Aust. J. Phys.* **49**, 905 (1996).

[25] Pasquini, B., Scherer, S. and Drechsel, D. Generalized polarizabilities of the proton in a constituent quark model revisited *Phys. Rev. C* **63**, 025205 (2001).

[26] Gorchtein, M., Lorce, C., Pasquini, B., Vanderhaeghen, M. Light-front interpretation of Proton Generalized Polarizabilities *Phys. Rev. Lett.* **104**, 112001 (2010).

[27] Mornacchi, E. *et al.* Measurement of Compton scattering at MAMI for the extraction of the electric and magnetic polarizabilities of the proton *arXiv:2110.15691* , (2010)

[28] Bourgeois, P. *et al.* Measurements of the generalized electric and magnetic polarizabilities of the proton at low Q^2 using the VCS reaction *Phys. Rev. Lett.* **97**, 212001 (2006)

[29] Bourgeois, P. *et al.* Measurements of the generalized electric and magnetic polarizabilities of the proton at low Q^2 using the virtual Compton scattering reaction *Phys. Rev. C* **84**, 035206 (2011)

[30] Blomberg, A. *et al.* Virtual Compton Scattering measurements in the nucleon resonance region. *Eur. Phys. J. A* **55**, 182 (2019).

[31] Pohl, R. *et al.* The size of the proton *Nature* **466**, 213-216 (2010)

[32] Antognini, A. *et al.* Proton structure from the mea-surement of 2S–2P transition frequencies of muonic hydrogen *Science* **339**, 417–420 (2013)

[33] Xiong, W. *et al.* A small proton charge radius from an electron–proton scattering experiment *Nature* **575**, 147–150 (2019)

[34] Fleurbaey, H. *et al.* New measurement of the 1S–3S transition frequency of hydrogen: contribution to the proton charge radius puzzle *Phys. Rev. Lett.* **120**, 182001 (2018)

[35] Bezginov, N. *et al.* A measurement of the atomic hydrogen Lamb shift and the proton charge radius *Science* **365**, 1007 (2019)

[36] Bernauer, J. C. *et al.* High-Precision Determinatio nof the Electric and Magnetic Form Factors of the Proton *Phys. Rev. Lett.* **105**, 242001 (2010)

[37] Atac, H. *et al.* Charge radii of the nucleon from its flavor dependent Dirac form factors *Eur. Phys. J. A* **57**, 65 (2021)

[38] Grinin, A. *et al.* Two-photon frequency comb spectroscopy of atomic hydrogen *Science* **370**, 1061–1066 (2020)

[39] Atac, H. *et al.* Measurement of the neutron charge radius and the role of its constituents *Nature Commun.* **12**, 1759 (2021)

[40] H. Atac et al., arXiv:2308.07197

[41] B. Pasquini and M. Vanderhaeghen, Eur. Phys. J. A 57 (2021) 11, 316